

**PROPERTIES OF LUNAR CRATER EJECTA FROM NEW 70-CM RADAR OBSERVATIONS.** R.R. Ghent<sup>1</sup>, D.W. Leverington<sup>1</sup>, B.A. Campbell<sup>1</sup>, B.R. Hawke<sup>2</sup>, and D.B. Campbell<sup>3</sup>, <sup>1</sup>Center for Earth and Planetary Studies, Smithsonian Institution, Washington, DC 20013-7012, <sup>2</sup>University of Hawaii, Honolulu, HI 96822, <sup>3</sup>Cornell University, Ithaca, NY 14853. (ghentr@nasm.si.edu),

**Introduction:** We use recently acquired radar observations at 70-cm wavelength to examine the distribution of ejecta around lunar impact craters. Numerous craters with haloes characterized by low 70-cm radar return occur throughout the maria and highlands (Table 1) [1]. These haloes extend 1-2 crater diameters from the rim, outboard of a zone of radar-bright rough ejecta that varies in width between craters; in some instances the radar-dark halo reaches the rim of the crater. We focus here on Aristarchus and Petavius craters.

Two possible explanations for these haloes are examined. The low-return areas may indicate the presence of a regolith component with relatively high loss tangent. For the mare craters, this would imply a layer of higher-TiO<sub>2</sub> basalt within the underlying lava flow units. For the highland craters, this would require excavation of mare basalt and its incorporation into the terra regolith; the mixed deposit would have a lower total radar echo than pure highlands material. The second model involves a relatively block-free mantling deposit produced by the impact process [2]. The second model has advantages in that it does not require fortuitous subsurface deposits of high-loss materials in the target area. Thermal infrared observations of craters also support the mantling deposit hypothesis [3]. Both mechanisms may occur to varying degrees, however, depending upon the stratigraphy of the target site.

The new 70-cm radar observations allow detailed analysis of the backscatter variations associated with these dark haloes. Clementine multispectral data [4] are used to infer mineralogical and maturity properties. Taken together, these data permit development of a more robust model for the physical and chemical partitioning of ejecta deposits.

**Radar data:** The 70-cm radar data presented here were collected at Arecibo Observatory. The Arecibo system permits measurement only of the cross-polarized circular (LR) echo; recent observations use the Greenbank telescope to receive both echo polarizations. Spatial resolution is 300-400 m, and a total of 5-8 looks are collected for each target. The 70-cm radar signals penetrate up to several meters in mare materials, and up to perhaps 8 m in low-loss highland regolith. These data thus probe a much greater regolith volume than multi-spectral measurements. Subsurface returns are modulated by

the regolith loss tangent, which varies with the abundance of lossy minerals such as ilmenite. Earlier radar observations at 3.8 and 12.6 cm wavelengths are also available for some areas [5, 6, 7].

**Aristarchus:** A comparison between the radar images and Clementine, Lunar Orbiter, and Apollo Panoramic Camera data is presently underway. Of particular interest are spatial patterns of low 70-cm radar return (Fig. 1) that are not immediately apparent in the multispectral data (Fig. 2), such as the dark “spokes” emanating radially from Aristarchus toward the south and east. Close examination of all the available data will aid in distinguishing between compositional and block size variations as the cause for the low radar returns.

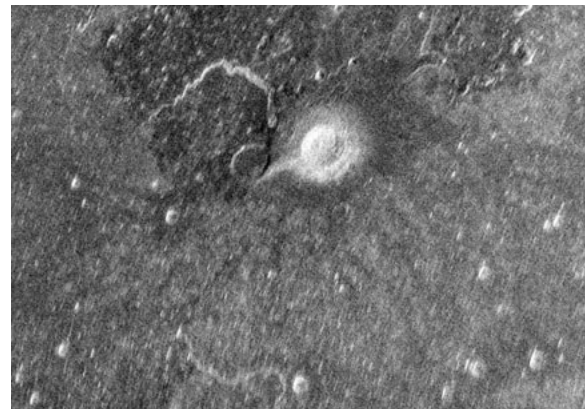


**Figure 1.** 70 cm radar image of the Aristarchus region. Note the low-radar-return halo surrounding the proximal bright ejecta, and low-return radial “spokes” to the south and east. 300-m resolution.

**Petavius:** New 70-cm data for Petavius will be collected in the coming year, so at present we are analyzing earlier 3-km resolution images (Fig. 3) [8]. These data show that Petavius has a nearly symmetric concentric annulus of low radar return, overlain in several locations by the rough ejecta of younger craters. Preliminary analysis of Clementine data shows little correlation between the area of low radar return and variations in near-infrared reflectance ratios. This suggests that the low radar return is due to a layer of rock-poor ejecta, but additional work is required to confirm this model.

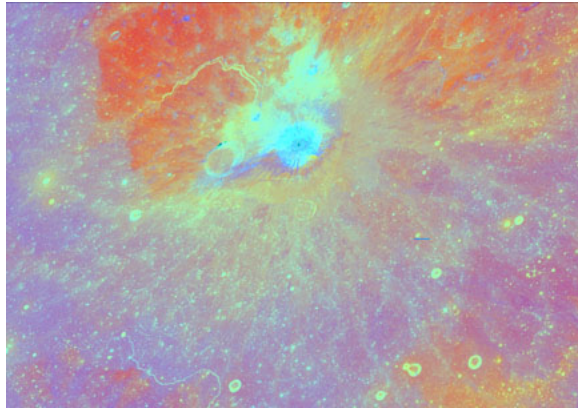


**Figure 2.** Clementine multispectral composite image of the region shown in Fig. 1. Colors correspond to band ratios: r: 750/415 nm, g: 750/1000 nm, b: 415/750 nm.

**Implications:** While our analysis is ongoing, it is clear that physical (i.e., block size) variations are likely responsible for the low radar return at 70 cm, as the surficial mineralogical signature of distal crater ejecta does not reflect the same pattern. Our lunar work thus has application to thermal infrared observations of craters on Mars, and potentially for interpretation of Messenger data for Mercury.



**Figure 3.** 70-cm radar image of Petavius crater and surrounding region. 3 km spatial resolution.

**References:** [1] Thompson, *The Moon*, 10, 51-85, 1974; [2] Oberbeck, *Rev. Geophys.*, 13, 337-362, 1975.; [3] Schultz and Mendell, 1978. *Proc. Lunar Planet. Sci. Conf. 9<sup>th</sup>*, 2857-2883; [4] McEwen, A., et al., *Science*, 266, 1858-1862, 1994; [5] Zisk, S.H., et al., 1974. *The Moon*, 10, 17-50; [6] Zisk, S.H. et al., *The Moon*, 17, 59-99, 1977; [7] Stacy N.J.S., Ph.D. Thesis, Ithaca, NY: Cornell University, 1993; [8] Thompson, T.W., *Earth, Moon, and Planets*, 37, 59-70, 1987.

**TABLE 1.** List of nearside craters with surrounding areas of low 70-cm radar return.

Crater	Location (Lat, Lon)	Type of Feature
<b>Mare Craters:</b>		
Aristoteles	50.4 N, 16.9 E	Mare Frigoris; halo darker than surrounding area
Galle	56.1 N, 21.9 E	Mare Frigoris; halo darker than surrounding area
Peirce	18.9 N, 53.4 E	Mare Crisium; halo darker than surrounding area
Picard	15.2 N, 54.6 E	Mare Crisium; halo darker than surrounding area
Piazz-Smyth	42.3 N, 3.5 W	Small dark-haloed crater
Bessel	22.4 N, 17.9 E	Low-return oblong area which splits into two lobes
Delisle/Diophantus	29.8 N, 34.6 W; 27.4 N, 34.1 W	Low-return area surrounds both craters
Krafft/Cardanus	16.3 N, 72.7 W; 13.1 N, 72.5 W	Low-return arc to west of both craters
Galilaei and Galilaei A	11.0 N, 63.0 W	Small dark halo surrounds both craters
Reiner	6.8 N, 54.9 W	Oblong dark halo oriented NW-SE
Bullialdus	21.0 S, 22.8 W	Slight darkening around crater
Taurantius	6.0 N, 46.4 E	Very weakly defined halo
Aristillus	33.9 N, 1.0 E	Surrounded by dark mare; may be fortuitous
Timocharis	26.8 N, 13.5 W	Surrounded by dark mare; may be fortuitous
Briggs/Russell	26.5 N, 69.3 W; 28.0 N, 71.0 W	Surrounded by dark mare; may be fortuitous
Burg	45.6 N, 27.9 E	Lacus Mortis; "halo" identification uncertain
<b>Mixed or Highland Craters:</b>		
Hercules/Atlas	41.4 N, 47.2 E	Appear to have mixed mare into highlands nearby
Plato	51.7 N, 9.8 W	Surrounded by low-return areas in the Jura Mts.
Aristarchus	23.6 N, 47.6W	Low-return wedge N and E of crater, radial spokes S and E
Petavius	25.0 S, 60.6 E	Radar dark ejecta on surrounding highlands terrain
Theophilus	10.9 S, 26.4 E	Low-return halo on mare side of target area only
Hainzel	40.1 S, 34.5 W	Low-return halo in surrounding highlands
Schluter	5.3 S, 83.4 W	Oblong dark halo in highlands